THE DESIGN AND ASSESSMENT OF DAMMAR GUM NANOPARTICLES CONTAINING MORONIC ACID AND TAMOXIFEN FOR CANCER TREATMENT

Deepshikha Verma[1], Neeraj Sethi[2*], Ashish Narain Dubey[3]

Abstract

The management of cancer often involves therapeutic techniques that are frequently associated with drug tolerance or multidrug resistance. The effectiveness of plant secondary metabolites in fighting cancer can be significantly increased by synthesizing them at the nanometric scale. Moronic acid (MA) is a type of pentacyclic triterpenoid that hinders the regulation of cell growth, hence reducing the multiplication of cancer cells. Tamoxifen (TAM) is a supplementary compound used in the hormonal treatment of cancer, particularly breast cancer. In this study, we used the oil in oil (O/O) emulsion solvent evaporation method to synthesize Dammar gum nanoparticles (MTDNPs) loaded with MA and TAM. This was done to enhance the bioavailability and synergism of the nanoparticles. The zeta potential of MTDNPs was determined to be +23 mV, indicating the nanoformulations relative stability. The encapsulation efficiency values were determined to be 72.5% for MA and 76.6% for TAM. The MTDNPs exhibit a particle size ranging from 45 to 55 nm, as observed using transmission electron microscopy. The MTDNPs exhibited a continuous release pattern, and their antioxidant and anticancer capabilities were significantly stronger compared to the individual MA and TAM particles in their free form. The in vitro tests revealed that the combination of MA and TAM, encapsulated in dammar gum, exhibited a stronger inhibitory effect on the growth of A-549, MCF-7, and Hela cell lines compared to the individual administration of MA and TAM. This finding confirms the potent anticancer properties of the encapsulated compounds.

Keywords: Dammar gum, Moronic acid, Tamoxifen, Anti-cancer, Nanoparticles

[1,3]Department of Chemistry, NIILM University, Kaithal,
Email: deepshikhavk24@gmail.com[1], andubey1977@gmail.com[3]
[2*]Department of Biotechnology, OSGU, Hisar, 20neerajsethi@gmail.com

***Corresponding Author:** Neeraj Sethi
Email:20neerajsethi@gmail.com

DOI: - 10.53555/ecb/2024.13.01.36

Introduction

Cancer nanotechnology is a burgeoning field of medicinal research. Nanotechnology facilitates the creation of innovative nanoplatforms filled with bioactive substances for the purpose of combating cancer. The administration of chemotherapy, in combination with cytotoxic drugs, is commonly employed for the treatment of many types of malignancies [1]. On the other hand, these traditional healing methods are associated with harsh consequences, specifically the development of drug tolerance or resistance [2, 3]. Currently, there is a growing popularity in the use of nanotechnology to develop remedies for life-threatening disorders. The bioactive agents at nanometric size exhibit great bioavailability at low dose and increased antioxidant and anticancer properties. The National Institute of Cancer in the United States has advocated for the investigation of the anticancer properties of several plant secondary metabolites [4,5]. Phytochemicals such as boswellic acid, moronic acid and ursolic acid have demonstrated cytotoxic effects [6]. Recent research has demonstrated that the physical characteristics of nanoparticles play a crucial role in achieving effective cancer-fighting activities while minimizing adverse effects [7]. The size, shape, and surface characteristics of nanoparticles have an impact on both the pharmacokinetic and pharmacodynamic qualities.

Moronic acid (MA), a pentacyclic triterpenoid, is found either as the aglycone of saponins or as a free carboxylic acid [8]. The presence of glucocorticoids causes a transformation of glucocorticoid receptors, resulting in a decrease in Bcl2 (anti-apoptotic proteins) in human breast cancer cell lines (Michigan Cancer Foundation-7) [9, 10]. MA is commonly utilised in pharmaceutical formulations for both oral and topical administration due to its low toxicity level [11]. The LD50 values for MA were determined to be 637 mg/kg (intraperitoneal administration) and 8330 mg/kg (oral administration) during acute toxicity studies conducted in mice [12].

When selecting an agent to encapsulate several medications, it is essential to consider biodegradability and biocompatibility as important properties [13, 14]. Dammar gum is a new chemical used for encapsulating therapeutic substances. It has been observed that the efficiency of encapsulation increases proportionally with higher concentrations of gum [15].

Tamoxifen (TAM) is a selective intracellular modulator of the estrogen receptor, prescribed for the treatment of breast cancer [16, 17]. This chemical is nonpolar and works by competitively blocking estrogen receptors to inhibit the development of cancer cells [18-20]. The particular structure of this substance allows it to interact with the cell membrane and enhance the effectiveness of hormone therapy against cancer. However, it also has associated side effects. [21]

The objective of this study was to enhance the bioavailability of moronic acid (MA) by co-delivering it with TAM polymeric nanoplatform. This approach was also aimed at mitigating negative effects and achieving synergistic effects. The incorporation of TAM and MA within the polymeric nanoparticles results in a controlled and prolonged release, leading to enhanced therapeutic effectiveness even at low doses.

Experimental Details

Materials

The drug Tamoxifen and gum dammar were purchased from MP Biomedicals, LLC, which is located in France. Moronic acid was purchased from Sigma Aldrich that is located in India. On the other hand, Minimum Essential Eagle Medium, Foetal bovine serum (FBS), penicillin, and streptomycin were purchased from Hi-media Laboratories Pvt. Ltd. that is located in Mumbai, India. The National Centre for Cell Science (NCCS) in Pune was the source of the cell lines—specifically, A-549 (human lung adenocarcinoma epithelial cells), MCF-7 (human breast adenocarcinoma cells), and Hela (human cervical carcinoma cell line)—that were used in this study. In the current experiment, the chemicals that were used were of the analytical reagent grade.

Preparation of MA & TAM loaded dammar gum nanoparticles (MTDNPs)

A process known as oil in oil emulsion solvent evaporation was utilised in order to produce the MTDNPs. 120 ml of n-butanol was used to dissolve 200 mg of dammar gum, 100 mg of moronic acid, and 20 mg of Tamoxifen. The mentioned solution was given 25 mgs of magnesium stearate, and the resulting combination was held under magnetic stirring at a speed of one thousand revolutions per minute for 1 hour. Continuous stirring was performed at 1000 rpm at 42 degrees Celsius for 60 mins, then the mixture was centrifuged at 9000 revolutions per minute at 4 degrees Celsius for 30 mins. Following the collection of the pellet, it was freeze-dried after being suspended in cryoprotectant (D-Mannitol, 5% weight-to-volume).

Characterization of synthesized MTDNPs

For the purpose of determining the average size and size distribution (polydispersity index) of the optimized nanoformulation of MTDNPs, a Zetasizer Nano ZS-90 produced by Malvern Instruments in Malvern, United Kingdom was utilised. A supernatant containing the unbound drug was collected and analyzed by high-performance liquid chromatography (HPLC) after centrifugation at 9000 revolutions per minute (four degrees Celsius) for thirty minutes. The following formula was used to compute the percentage of encapsulation efficiency:

The transmission electron microscope (TEM-Hitachi-H-7501SSP/N-817-0520, Japan) was used to examine the size and morphology of the optimized batch of UTDNPs. The magnification factor was set to 60,000, and the accelerating voltage was set to 80,000V. Using the TGA/DSC 3+ Star System, which was manufactured by Mettler Toledo AG, Analytical, Switzerland, a differential scanning calorimetry-thermogravimetric analysis (DSC-TGA) was carried out on MTDNPs and dummy nanoparticles in order to ascertain the nature of the physical interaction that exists between MA, TAM, and dammar gum. A variety of samples, each weighing 5 mgs, were collected in a pan made of aluminum and subjected to scanning at temperatures ranging from 30 degrees Celsius to 500 degrees Celsius, with a heat flow rate of 15 degrees Celsius per minute. The Fourier transform infrared spectrophotometer (FTIR Affinity-1, Shimadzu, Japan) was utilised to conduct the FTIR analysis of MA, TAM, Dammar gum, and MTDNPs. The spectrophotometer was set to operate within the range of 4500–500 cm^{-1}.

In vitro release profile of MTDNPs

The dialysis sac method was employed to investigate the release profile. A total of 10 mg of tamoxifen-loaded dammar gum nanoparticles, co-delivered with moronic acid, were placed into a dialysis sac. The sac was then submerged in a solution consisting of 10 ml of water, 25% ethanol, and 0.1 M phosphate buffer saline at a pH of 7.4. The solution was continuously swirled at a rate of 100 revolutions per minute, while maintaining a constant temperature of 37 °C. A 1 ml sample was taken at regular intervals of 1, 2, 3, 6, 12, and 24 hours and analysed using High Performance Liquid Chromatography (HPLC) with an Agilent 1200 Infinity Series instrument. The analysis was performed using a ZORBAX SB C-18 column (5 µm, 150 x 4.6 mm) and a mobile phase consisting of Acetonitrile: Water (80:20 v/v). The compounds of interest, MA and TAM, were detected at wavelengths of 210 nm and 254 nm, respectively, with retention times of 6.28 minutes and 7.23 minutes.

Antioxidant activity

The antioxidant capacity of MA, TAM, Dammar Gum, and MTDNPs was assessed using the DPPH assay. The compound 1,1-diphenyl-2-picrylhydrazyl (DPPH), which is a type of free radical, was completely dissolved in methanol at a concentration of 3.9 mg per 100 ml. The samples of pure MA, TAM, Dammar Gum, and MTDNPs were mixed with DPPH and left in the dark for 30 minutes. This was done in triplicate to ensure accuracy. The absorbance of the mixture was then measured using a UV spectrophotometer at a wavelength of 517 nm to quantify the extent of DPPH inhibition. Blank Dammar NPs were utilised as a negative control, however pure moronic acid and TAM were applied as positive controls. The % inhibition of DPPH by pure MA, TAM, and MTDNPs was determined using the following formula:

$$\text{Percent antioxidant activity} = \frac{\text{Absorbance of control- Absorbance of sample}}{\text{Absorbance of control}} \times 100$$

In-vitro assay for cytotoxic activity (MTT assay)

Both normal and cancer cell lines were cultivated in media containing inactivated foetal bovine serum (10%), streptomycin (100µl/ml), and penicillin (100µl/ml). The cells were then incubated at a temperature of 37°C with a 5% concentration of carbon dioxide. Once the cells reached a confluence of 75%, they were transferred to a sterile environment and sub-cultured using a 0.25% trypsin solution. The compounds and standards were produced as stock solutions in DMSO at a concentration of µM/ml. Subsequently, dilutions were made in the medium at concentrations of 1µM, 10µM, 20µM, 50µM, and 100µM per ml. The cells were seeded in 96-well plates at a density of 5×103 cells per 100µl per well. The density of each cell line was assessed based on their growth parameters. The wells were subjected to treatment with varying concentrations of MTDNPs (0.1-1000µg/ml) and moronic acid for a duration of three days (in triplicate) following an incubation period of 8 hours. Following a three-day treatment period, the medium was substituted with 3µl of MTT solution (5mg/ml) and let to incubate

for 3 hours. The percentage of cells exhibiting metabolic activity was compared to untreated control cells based on the conversion of 3-(4, 5-dimethylthiazol-2-yl) 2, 5 diphenyltetrazolium bromide (MTT) into Formazan crystals by mitochondria. The formazan crystals were solubilized in dimethyl sulfoxide (DMSO) and the absorbance was measured at 570 nm using a microplate reader. The anti-cancer efficacy of UTDNPs was assessed using pure MA and TAM as reference standards by MTT test on three cell lines: A-549 (human lung adenocarcinoma epithelial cells), MCF-7 (human breast adenocarcinoma cells), and Hela (human cervical carcinoma cell line). The percentage of cell growth inhibition (1) and cytotoxicity (2) was determined using the following formula:

%viability = $(A_{Tr} - A_{Bl}) / (A_{Ct} - A_{Bl}) \times 100$ ……. (1)

Where A_{Tr} = Absorbance for treated cells (drug); A_{Bl} = Absorbance for blank

A_{Ct} = Absorbance for control (untreated)

%cytotoxicity = 100 – Percent cell survival (%) ……. (2)

Results and Discussion

Particle size and Zeta Potential

An analysis was conducted on the MTDNPs to determine their particle size and zeta potential. The size of the MTDNPs was determined to be 148 nm (Fig 1), and the zeta potential was measured to be +23 mV (Fig 2), indicating the relative stability of the generated nanoformulation.

Percent encapsulation efficiency

The efficacy of encapsulation is contingent upon the specific molecule, process, encapsulating materials, and media used for synthesizing nanoparticles [22]. The encapsulation efficiency percentage was determined by analyzing the supernatant using HPLC to measure the amount of unbound medication. The results showed an encapsulation efficiency of 72.5% for MA and 76.6% for TAM (Fig 5). Both Moronic acid and Tamoxifen have hydrophobic properties. They have excellent solubility in gum solution that is produced using n-butanol. Because dammar gum is hydrophobic (nonpolar), it exhibited a significant attraction to both MA and TAM. As a result of this attraction, the medication was more effectively encapsulated in dammar gum.

Morphological characterization of **MTDNPs** *by TEM*

The UTDNPs were separated and had a consistent spherical shape, as observed using Transmission Electron Microscopy (Fig 3). Their size ranged from 45 to 55 nm. The nanoparticles' size was seen to vary using PSA and TEM. PSA considers the fluidized ionic environment around the nanoparticles, while TEM measures the size of the particles in a dry and isolated atmosphere, resulting in particle shrinkage. The release rate of nanoparticles is influenced by their size [23, 24]. Nanoparticles are distributed to various organs in the body based on their morphology and dimensions. The form and size of nanoparticles play a crucial role in determining their stability, biocompatibility, and capacity to penetrate cell tissues [25]. Nanoparticles of smaller dimensions exhibit prolonged retention in the systemic circulation as compared to nanoparticles of larger dimensions [26].

FTIR Analysis of Drug Samples

FTIR spectroscopy is employed for both investigating the interaction studies [27] and assessing the nanoencapsulation of bioactive compounds [28]. Figure 4 displays the FTIR spectra of the individual components: pure drug MA, TAM, dammar gum, and MTDNPs. The MA FTIR spectrum exhibits absorption peaks at 3234 cm^{-1} corresponding to the -OH group, and at 2897.0 cm^{-1} and 2244 cm^{-1} for the terminal –CH3 groups. The FTIR spectra of Tamoxifen (TAM) in Figure 4B has a distinctive absorption band at 2811 cm-1 for =C-H stretching and at 1600 cm^{-1} for C=C ring stretching. The wavenumber values of 1345 cm^{-1} and 3453 cm^{-1} indicate the stretching of -NH2. The FTIR spectrum of dammar gum, as depicted in Figure 4 C, exhibits a peak at 3346 cm^{-1}, which corresponds to the stretching of –OH groups, and a peak at 2845 cm^{-1}, indicating the stretching of aliphatic –CH groups in dammar gum. The FTIR spectra of MTDNPs, as depicted in Figure 4D, exhibits changes at wave numbers of 3400 cm^{-1}, 1434 cm^{-1}, 2453 cm^{-1}, and 2871 cm^{-1}. This region corresponds to the infrared stretching vibration range of functional groups such as hydroxyl (-OH), double bond (C=C) stretching, methyl group (-CH3) stretching, and carbon-hydrogen (C-H) stretching. Weak intermolecular forces, such as dipole-dipole interactions, hydrogen bonding (between hydrogen and electronegative atoms like N, O, F), and weak Van der Waals forces (which depend on mass), occur between the C-H groups in the drug molecule and OH groups in dammar gum. The medications and excipients exhibit distinct peaks in the FTIR spectrum. The peak strength decreased and the bands shifted, indicating the

presence of chemical interaction between tamoxifen, moronic acid, and dammar gum.

In-vitro drug release

Continuous nanoparticle bioactive chemical liberation protects it against quick metabolism and degradation [29]. MA, TAM, and MTDNP in vitro drug release is shown in Figure 6. In-vitro drug release data shows 95% of pure MA and 98% of pure TAM released within 4 hours. Due to dammar gum emulsification, MTDNPs release the drug sustainably. One hour after treatment, MTDNPs release 20% MA and 18.6% TAM. Within 24 hours, MTDNPs released 80% MA and 85% TAM. Hydrophobic (nonpolar) MA and TAM allow MTDNPs to release MA and TAM over time. Dammar gum formed a cohesive matrix around MA and TAM particles, ensuring their prolonged release.

DSC Analysis

The DSC thermogram of free tamoxifen shows a lower intensity endothermic peak and progress crests at 150˚C, indicating the drug. Free moronic acid DSC thermograms show two endothermic peaks. The initial endothermic peak at 286˚C, despite its low intensity, suggests moronic acid [30]. The abrupt, intense peak confirmed crystalline nature. All DSC graph crests were not sharp, indicating that nanoformulation is amorphous and that drug was appropriate for amorphous nature. Moronic acid co-delivered tamoxifen-loaded dammar gum nanoparticles exhibit a low intensity endothermic peak crest at nearly 374˚C, indicating amorphous behaviour where primary decomposition begins at 318˚C and secondary decomposition occurs at 445˚C. The low-intensity, blunt peak hump confirms its amorphous character. The DSC thermogram of blank dammar gum nanoformulation shows two endothermic pinnacles (Fig 7 A), with the first peak at about 178˚C and low force. The second endothermic peak was about 374˚C, indicating breakdown after that temperature. Its low force and blunt peak confirmed its amorphousness. Compared to MTDNPs, dummy nanoformulation has a modest liquefying endotherm movement (Fig 7 B). The melting point peak of MA-TAM loaded dammar gum nanoparticles shifted higher, indicating co-amorphous phase formation.

Thermo-gravimetric analytical studies

Maximal weight reduction of dummy dammar nanoformulation occurred at 359˚C. MTDNPs showed considerable melting endotherm movement compared to dummy dammar gum nanoformulation, with the highest weight loss at 412˚C.These results indicate that co-amorphous phase development differed between MA and TAM entrapped dammar gum nanoformulation and dummy nanoformulation (Fig 7).

Anti-oxidant activity

DPPH assay quantifies encapsulated molecular antioxidant activity [31]. DPPH (1,1-diphenyl-2-picrylhydrazyl) is a persistent free radical with spare electrons distributed throughout the molecule, giving it a deep violet colour. Absorption occurs around 517 nm [32]. DPPH solutions uniformly mixed with hydrogen-donating molecules lose their violet colour. MA and TAM are well-known antioxidants. Incubating antioxidant molecules MA and TAM with DPPH (a hydrogen atom donor) produced a stable non-radical version of DPPH that turned violet to pale yellow. Thus, absorption band decreased. Labile hydrogen atoms in MA and TAM block DPPH when released. Due to their nanometric dimension, MTDNPs inhibited DPPH as more than MA and TAM alone during dark incubation, protecting them from oxidation (Fig 8).

Anti-cancer activity

Nanoparticles are cytotoxic because their vast surface area allows drug delivery and anticancer potential [33]. Nanoparticles of 100 nm size can easily permeate tumor cells by retention and vascular permeation [34]. NPs' anticancer effects depend on size [35,40]. Small nanoparticles can better penetrate tumors. The enzyme mitochondrial dehydrogenase is found in living cells. It breaks the pale-yellow tetrazolium ring structure of MTT dye to generate dark purple formazan crystals that accumulate in cells [41-48]. The present investigation indicated that MTDNPs had better anti-cancer effectiveness than pure active medication. In vitro, dammar gum-encapsulated MA and TAM suppressed A-549, MCF-7, and Hela cell proliferation better than the free medicines. Table 1 shows the IC50 values (µg/ml) of synthesized nanoparticles and reference drugs tamoxifen and moronic acid. Compared to standard medications TAM and MA alone, MTDNPs showed powerful anticancer effects with IC50s of 4.1, 3.8, and 4.2 µg/ml against A-549, MCF-7, and Hela cell lines by optical microscopy. The synergistic impact of TAM and MA in MTDNPs caused their powerful anticancer effect.

Conclusions

The use of nanotechnology has greatly enhanced formulation research and development, which in turn has improved the likelihood of successfully addressing and treating diseases. Thanks to advancements in nano-drug delivery methods, researchers in the field of oncology are able to explore the combined effects of medications by

delivering nanoparticles with larger payloads, such as dual drug delivery. Drug tolerance/resistance, poor bioavailability, and short drug residence time are the main obstacles for these agents, even though many anticancer medicines have been discovered. Solubility, bioavailability, therapeutic potential, and adverse effect profiles can all be improved with the development of new nanoformulations that incorporate more potent excipients. Based on the results of this investigation, a new nanoformulation including moronic acid co-delivered tamoxifen loaded dammar gum nanoparticles is a strong contender for the fight against cancer due to its synergistic antioxidant and anticancer properties.

Conflict of Interest

There is no conflict of interest whatever.

REFERENCES

1. Wong, H.L., Bendayan, R., Rauth, A.M., Xue, H.Y., Babakhanian, K. and Wu, X.Y., 2006. A mechanistic study of enhanced doxorubicin uptake and retention in multidrug resistant breast cancer cells using a polymer-lipid hybrid nanoparticle system. *Journal of Pharmacology and Experimental Therapeutics*, *317*(3), pp.1372-1381.
2. Gottesman, M.M., Fojo, T. and Bates, S.E., 2002. Multidrug resistance in cancer: role of ATP–dependent transporters. *Nature Reviews Cancer*, *2*(1), pp.48-58.
3. Szakács, G., Paterson, J.K., Ludwig, J.A., Booth-Genthe, C. and Gottesman, M.M., 2006. Targeting multidrug resistance in cancer. *Nature reviews Drug discovery*, *5*(3), pp.219-234.
4. Sethi, N., Bhardwaj, P., Kumar, S., & Dilbaghi, N. (2019). Development and Evaluation of Ursolic Acid Co-Delivered Tamoxifen Loaded Dammar Gum Nanoparticles to Combat Cancer. *Advanced Science, Engineering and Medicine*, *11*(11), 1115-1124.
5. Sethi, N., Bhardwaj, P., Kumar, S., & Dilbaghi, N. (2019). Development And Evaluation Of Ursolic Acid Loaded Eudragit-E Nanocarrier For Cancer Therapy. *International Journal of Pharmaceutical Research (09752366)*, *11*(2).
6. Saini, A., Budania, L. S., Berwal, A., & Sethi, S. K. N. (2023). Screening of the Anticancer Potential of Lycopene-Loaded Nanoliposomes. *Tuijin Jishu/Journal of Propulsion Technology*, *44*(4), 1372-1383.
7. Xu, M., Han, X., Xiong, H., Gao, Y., Xu, B., Zhu, G., & Li, J. (2023). Cancer nanomedicine: emerging strategies and therapeutic potentials. *Molecules*, *28*(13), 5145.
8. Dhanda, P., Sura, S., Lathar, S., Shoekand, N., Partishtha, H., & Sethi, N. (2022). Traditional, phytochemical, and biological aspects of Indian spider plant.
9. Kaura, S., Parle, M., Insa, R., Yadav, B. S., & Sethi, N. (2022). Neuroprotective effect of goat milk. *Small Ruminant Research*, *214*, 106748.
10. Parveen, N., Abourehab, M. A., Shukla, R., Thanikachalam, P. V., Jain, G. K., & Kesharwani, P. (2023). Immunoliposomes as an emerging nanocarrier for breast cancer therapy. European Polymer Journal, 184, 111781.
11. Kumar, R., Sethi, N., & Kaura, S. (2022). Bio-processing and analysis of mixed fruit wine manufactured using Aegle marmelos and Phoenix dactylifer.
12. Poonam, D., Sethi, N., Pal, M., Kaura, S., & Parle, M. (2014). Optimization of shoot multiplication media for micro propagation of Withania somnifera: an endangered medicinal plant. *Journal of Pharmaceutical and Scientific Innovation (JPSI)*, *3*(4), 340-343.
13. Suman, J., Neeraj, S., Rahul, J., & Sushila, K. (2014). Microbial synthesis of silver nanoparticles by Actinotalea sp. MTCC 10637. *American Journal of Phytomedicine and Clinical Therapeutics*, *2*, 1016-23.
14. Chehelgerdi, M., Chehelgerdi, M., Allela, O. Q. B., Pecho, R. D. C., Jayasankar, N., Rao, D. P., & Akhavan-Sigari, R. (2023). Progressing nanotechnology to improve targeted cancer treatment: overcoming hurdles in its clinical implementation. Molecular cancer, 22(1), 169.
15. Milind, P., Sushila, K., & Neeraj, S. (2013). Understanding gout beyond doubt. *International Research Journal of Pharmacy*, *4*(9), 25-34.
16. Moreddu, R. (2023). Nanotechnology and Cancer Bioelectricity: Bridging the Gap Between Biology and Translational Medicine. *Advanced Science*, 2304110.
17. Sethi, N., Kaura, S., Dilbaghi, N., Parle, M., & Pal, M. (2014). Garlic: A pungent wonder from nature. *International research journal of pharmacy*, *5*(7), 523-529.
18. Verma, R., Bhatt, S., Dutt, R., Kumar, M., Kaushik, D., & Gautam, R. K. (2023). Establishing Nanotechnology-Based Drug Development for Triple-Negative Breast Cancer Treatment. Drug and Therapy Development for Triple Negative Breast Cancer, 153-180.
19. Milind, P., Renu, K., & Kaura, S. (2013). Non-behavioral models of psychosis. *International Research Journal of Pharmacy*, *4*(8), 89-95.
20. Dash, S. R., & Kundu, C. N. (2023). Cancer-induced Pain Management by Nanotechnology-

based Approach. Current Pharmaceutical Biotechnology, 24(11), 1365-1375.
21. Kaura, S., & Parle, M. (2015). Anti-Alzheimer potential of green moong bean. *Int. J. Pharm. Sci. Rev. Res*, *37*(2), 178-182.
22. Li, H., Fu, Q., Muluh, T. A., Shinge, S. A. U., Fu, S., & Wu, J. (2023). The Application of Nanotechnology in Immunotherapy based Combinations for Cancer Treatment. Recent Patents on Anti-Cancer Drug Discovery, 18(1), 53-65.
23. Monga, S., Sethi, N., Kaura, S., Parle, M., & Lohan, S. (2014). Effect of 6-benzyl amino purine hormone on the shooting growth of Ocimum gratissimum. *L. International Research Journal of Pharmacy*, *5*(2), 106-108.
24. Sathe, A., Prajapati, B. G., & Bhattacharya, S. (2023). Understanding the charismatic potential of nanotechnology to treat skin carcinoma. Medical Oncology, 41(1), 22.
25. Milind, P., Bansal, N., & Kaura, S. (2014). Take soybean to remain evergreen. *International Research Journal of Pharmacy*, *5*(1), 1-6.
26. Abdel-Halim, A. H. (2023). Strategies for cancer therapy: targeting tumor microenvironment and nanotechnology-y. *Egyptian Pharmaceutical Journal*, *22*(2), 165-176.
27. Parle, M., Malik, J., & Kaura, S. (2013). Life style related health hazards. *Int. Res. J. Pharm*, *4*(11), 1-5.
28. Kumar, P., Mangla, B., Javed, S., Ahsan, W., Musyuni, P., Ahsan, A., & Aggarwal, G. (2023). Gefitinib: an updated review of its role in the cancer management, its nanotechnological interventions, recent patents and clinical trials. Recent Patents on Anti-Cancer Drug Discovery, 18(4), 448-469.
29. Li, J., Zhu, L., & Kwok, H. F. (2023). Nanotechnology-based approaches overcome lung cancer drug resistance through diagnosis and treatment. Drug Resistance Updates, 66, 100904.
30. Parle, M., & Kaura, S. (2013). Green chilli: A memory booster from nature. *Ann. Pharm. and Pharm. Sci*, *4*(1), 17-21.
31. Kaura, S., & Parle, M. (2017). Evaluation of nootropic potential of green peas in mice. *Journal of Applied Pharmaceutical Science*, *7*(5), 166-173.
32. Nevins, S., McLoughlin, C. D., Oliveros, A., Stein, J. B., Rashid, M. A., Hou, Y., ... & Lee, K. B. (2023). Nanotechnology Approaches for Prevention and Treatment of Chemotherapy-Induced Neurotoxicity, Neuropathy, and Cardiomyopathy in Breast and Ovarian Cancer Survivors. *Small*, 2300744.
33. Kaura, S., & Parle, M. (2017). Anti-ageing activity of moong bean sprouts. *International Journal of Pharmaceutical Sciences and Research*, *8*(10), 4318-4324.
34. Zheng, N., Yao, Z., Tao, S., Almadhor, A., Alqahtani, M. S., Ghoniem, R. M., ... & Li, S. (2023). Application of nanotechnology in breast cancer screening under obstetrics and gynecology through the use of CNN and ANFIS. Environmental Research, 234, 116414.
35. Meenakshi, P., Neeraj, S., Sushila, K., & Milind, P. (2014). Plant regeneration studies in Safed musli (Chlorophytum sp.). *Int J Res Ayuveda Pharm*, *5*, 195-98.
36. Zhang, P., Xiao, Y., Sun, X., Lin, X., Koo, S., Yaremenko, A. V., ... & Tao, W. (2023). Cancer nanomedicine toward clinical translation: Obstacles, opportunities, and future prospects. Med, 4(3), 147-167.
37. Song, J., Wang, Y., Song, Y., Chan, H., Bi, C., Yang, X., Yan, R., Wang, Y. and Zheng, Y., 2014. Development and characterisation of ursolic acid nanocrystals without stabiliser having improved dissolution rate and in vitro anticancer activity. *Aaps Pharmscitech*, *15*(1), pp.11-19.
38. Kumari, A., Yadav, S. K., Pakade, Y. B., Singh, B., & Yadav, S. C. (2010). Development of biodegradable nanoparticles for delivery of quercetin. *Colloids and Surfaces B: Biointerfaces*, *80*(2), pp.184-192.
39. Khuroo, T., Verma, D., Talegaonkar, S., Padhi, S., Panda, A.K. and Iqbal, Z., 2014. Topotecan–tamoxifen duple PLGA polymeric nanoparticles: investigation of in vitro, in vivo and cellular uptake potential. *International journal of pharmaceutics*, *473*(1-2), pp.384-394.
40. Song, J., Wang, Y., Song, Y., Chan, H., Bi, C., Yang, X., Yan, R., Wang, Y. and Zheng, Y., 2014. Development and characterisation of ursolic acid nanocrystals without stabiliser having improved dissolution rate and in vitro anticancer activity. *Aaps Pharmscitech*, *15*(1), pp.11-19.
41. Molyneux, P., 2004. The use of the stable free radical diphenylpicrylhydrazyl (DPPH) for estimating antioxidant activity. *Songklanakarin J. Sci. Technol*, *26*(2), pp.211-219.
42. Dahiya, S., Rani, R., Kumar, S., Dhingra, D. and Dilbaghi, N., 2017. Chitosan-gellan gum bipolymeric nanohydrogels—a potential nanocarrier for the delivery of epigallocatechin gallate. *BioNanoScience*, *7*(3), pp.508-520.

43. Rao, P.V., Nallappan, D., Madhavi, K., Rahman, S., Jun Wei, L. and Gan, S.H., 2016. Phytochemicals and biogenic metallic nanoparticles as anticancer agents. *Oxidative medicine and cellular longevity*, *2016*, pp 1-15.
44. Siegler, E.L., Kim, Y.J. and Wang, P., 2016. Nanomedicine targeting the tumor microenvironment: Therapeutic strategies to inhibit angiogenesis, remodel matrix, and modulate immune responses. *Journal of Cellular Immunotherapy*, *2*(2), pp.69-78.
45. Piktel, E., Niemirowicz, K., Wątek, M., Wollny, T., Deptuła, P. and Bucki, R., 2016. Recent insights in nanotechnology-based drugs and formulations designed for effective anti-cancer therapy. *Journal of nanobiotechnology*, *14*(1), pp.39-53.
46. Barua, S. and Mitragotri, S., 2014. Challenges associated with penetration of nanoparticles across cell and tissue barriers: a review of current status and future prospects. *Nano today*, *9*(2), pp.223-243.
47. Gerlier, D. and Thomasset, N., 1986. Use of MTT colorimetric assay to measure cell activation. *Journal of immunological methods*, *94*(1-2), pp.57-63.
48. Van Meerloo, J., Kaspers, G.J. and Cloos, J., 2011. Cell sensitivity assays: the MTT assay. In *Cancer cell culture 731*, pp. 237-245.

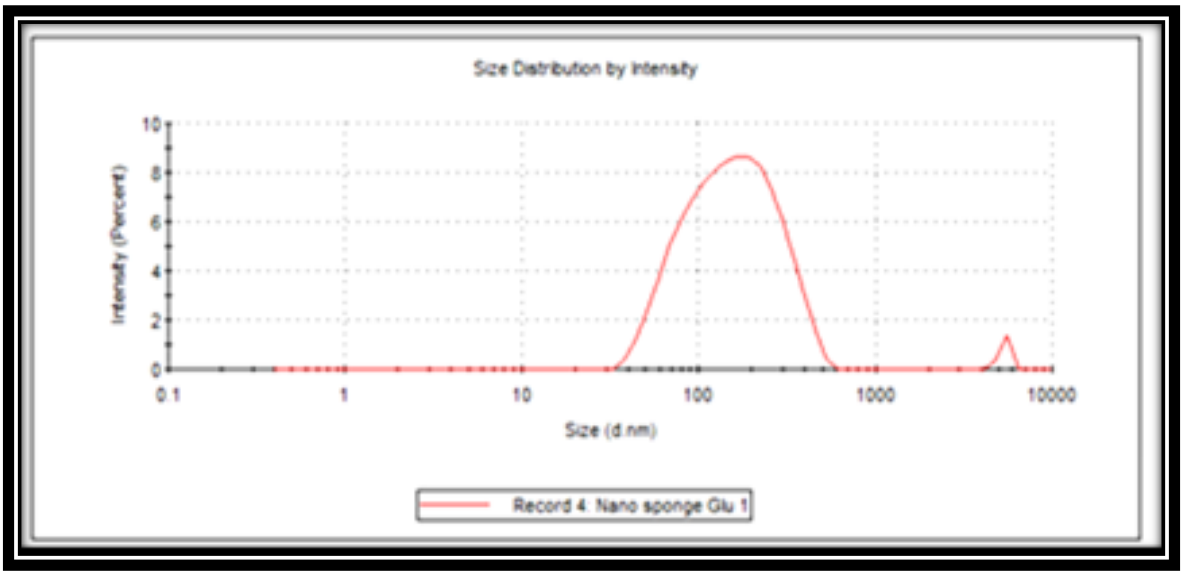

Figure 1. PSA image of MTDNPs

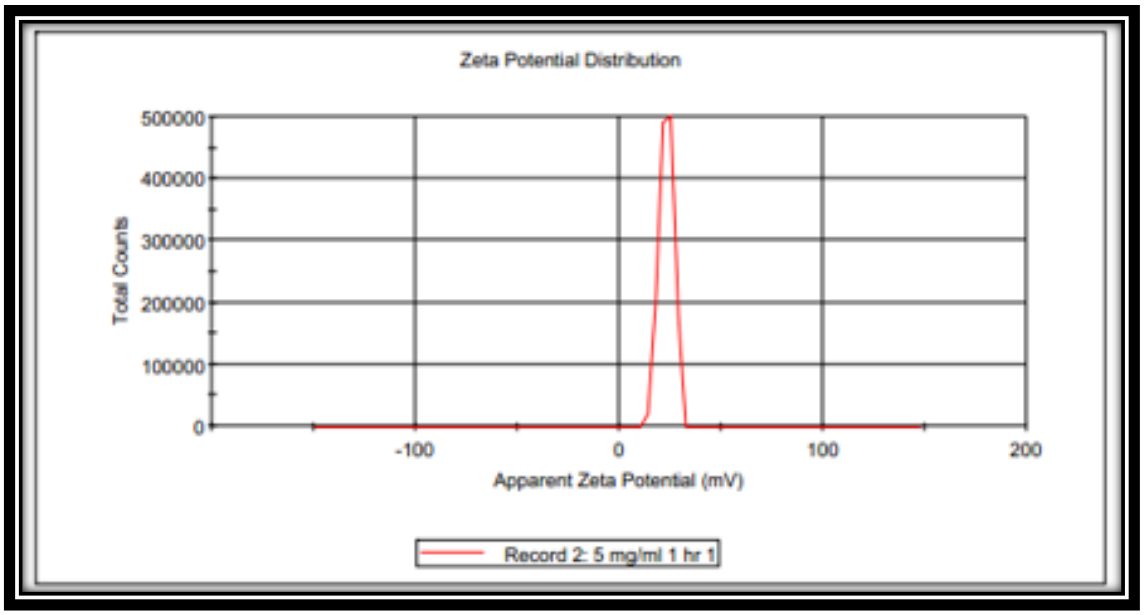

Figure 2. Zeta potential of MTDNPs

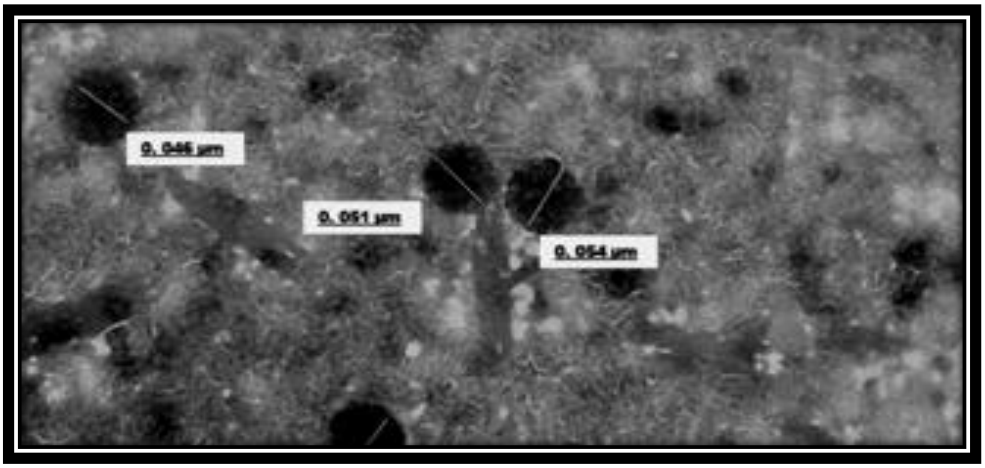

Figure 3: TEM image of MTDNPs

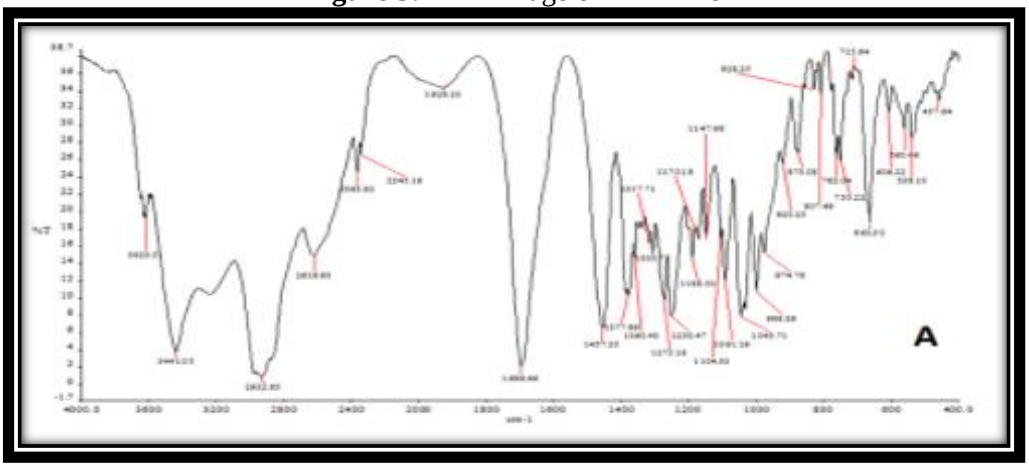

Figure 4. The FTIR spectra of (A) MTDNPs

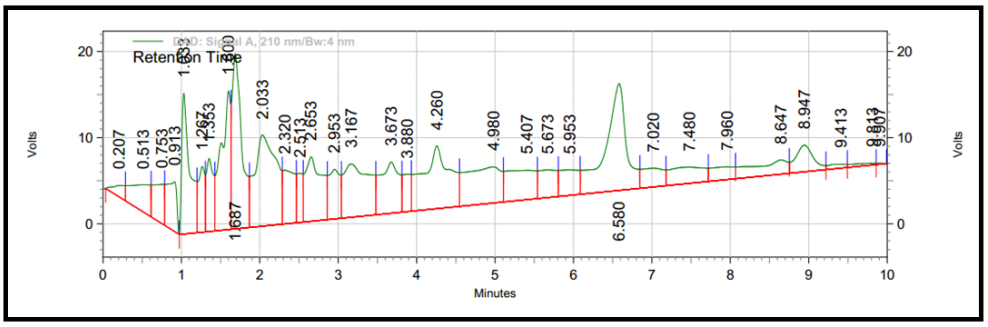

Figure 5. HPLC Chromatogram for supernatant

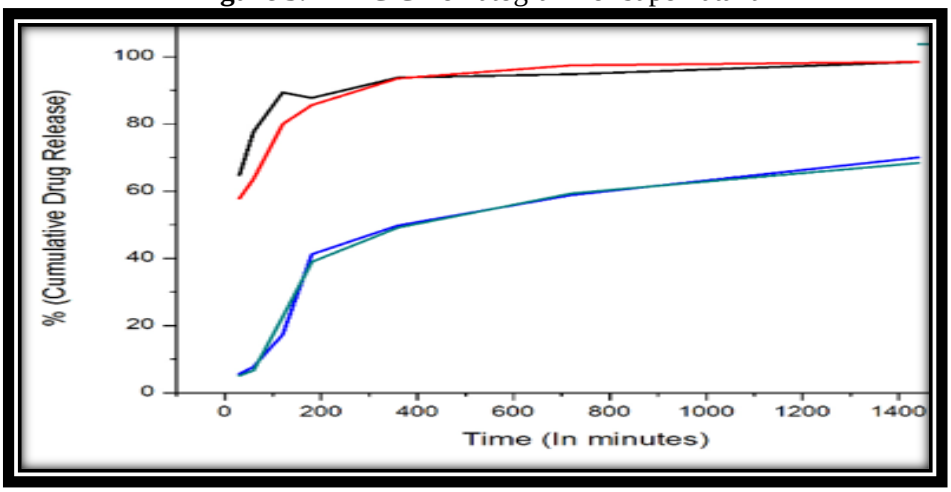

Figure 6. In-vitro release study

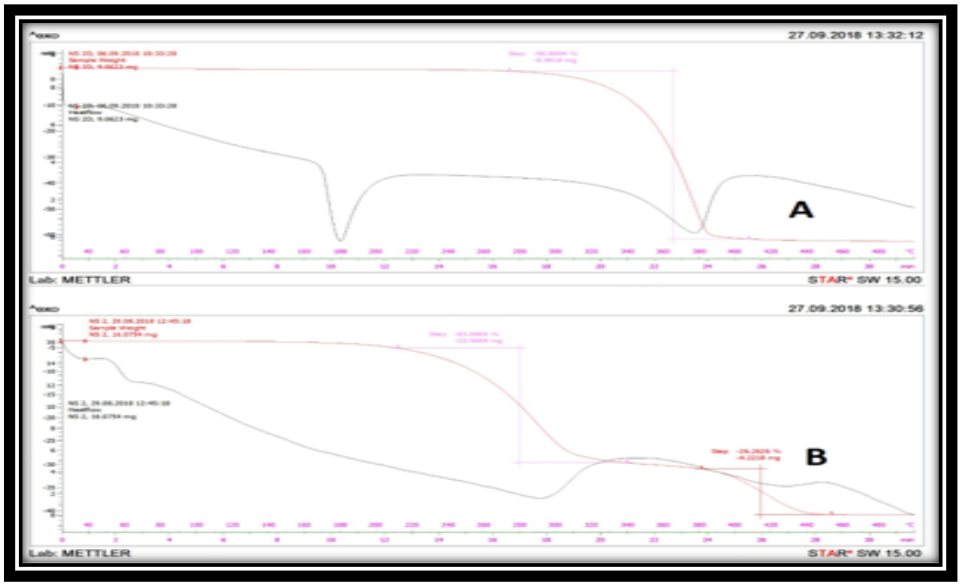

Figure 7. Differential Thermal Analysis (A) Blank Gum Dammar Nanoparticles

(B) Drug Loaded Gum Dammar Nanoparticles

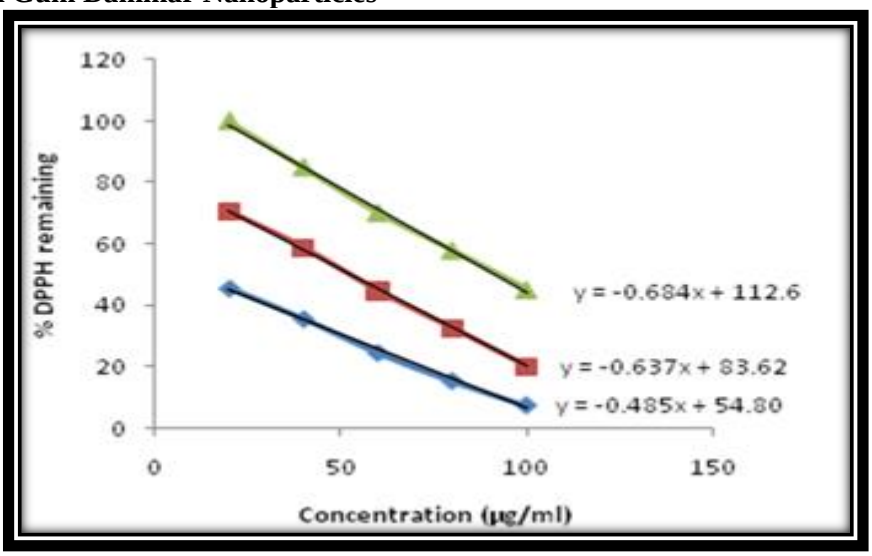

Figure 8. Antioxidant activity of MA, TAM and MTDNPs

Sample code	**A-549**		**MCF-7**		**Hela**	
	IC50	**pIC50**	**IC50**	**pIC50**	**IC50**	**pIC50**
Tamoxifen	6.2	-0.787341	5.2	-0.70827	5.3	-0.709838
Ursolic acid	27.45	-1.452732	27.23	-1.4503	30.11	-1.50187
UTDNPs	4.1	-0.643249	3.8	-0.58106	4.2	-0.618455

Table 1: IC50 values of MTDNPs along with standard drug tamoxifen and moronic acid